Chemical Science

EDGE ARTICLE

View Article Online
View Journal | View Issue

Cite this: *Chem. Sci.*, 2017, **8**, 1506

Green- to far-red-emitting fluorogenic tetrazine probes – synthetic access and no-wash protein imaging inside living cells†

Achim Wieczorek,‡ Philipp Werther,‡ Jonas Euchner‡ and Richard Wombacher*

Received 30th August 2016
Accepted 19th October 2016

DOI: 10.1039/c6sc03879d

www.rsc.org/chemicalscience

Fluorogenic probes for bioorthogonal labeling chemistry are highly beneficial to reduce background signal in fluorescence microscopy imaging. 1,2,4,5-Tetrazines are known substrates for the bioorthogonal inverse electron demand Diels–Alder reaction (DA_{inv}) and tetrazine substituted fluorophores can exhibit fluorogenic properties. Herein, we report the synthesis of a palette of novel fluorogenic tetrazine dyes derived from widely-used fluorophores that cover the entire emission range from green to far-red. We demonstrate the power of the new fluorogenic probes in fixed and live cell labeling experiments and present the first example of intracellular live cell protein imaging using tetrazine-based probes under no-wash conditions.

Introduction

Synthetic fluorophores represent a valuable alternative to fluorescent proteins for the labeling of biomolecules in living cells and organisms. They are much smaller in size and in general exhibit superior photophysical properties such as higher brightness and photostability.[1] However, the beneficial photophysical properties come with the disadvantage that applications of synthetic fluorophores in live cell experiments often suffer from unwanted background signal due to unbound fluorophore and unspecific localization. To overcome this problem, fluorophores can be equipped with a fluorescence-quenching moiety that is either chemically converted or eliminated in the labeling process. This leads to an fluorescence increase upon binding to the biomolecular target, which is why such molecules are referred to as fluorogenic probes.[2,3] In addition to reducing background signal, fluorogenic probes have the potential to be used in fluorescence microscopy experiments that do not tolerate excessive washing of the imaging sample. Fluorogenic probes are highly desirable when a specific biomolecule is to be selectively labeled in the presence of a plethora of biomolecules.

To date, a number of methods for selective biomolecule labeling have been reported including the use of protein tags,[4–6] peptide tags[6–8] and unnatural amino acids.[9,10] They often involve bioorthogonal chemical reactions like the copper catalyzed (CuAAC)[11,12] and strain-promoted azide alkyne cycloaddition (SPAAC)[13] as well as the inverse electron demand Diels–Alder cycloaddition (DA_{inv})[14,15] between 1,2,4,5-tetrazines and strained olefins. Fluorogenic variants exist for all of those reactions.[16–21]

Tetrazine-based fluorogenic probes[16–20] are particularly interesting as the tetrazine moiety within these molecules serves as reactive group and fluorescence quencher at the same time. Hence, conversion of the tetrazine in DA_{inv} results in the loss of its quenching properties. Existing reports of extracellular or intracellular biomolecule labeling with tetrazine fluorogenic probes were either conducted in fixed cells,[18] on cell surfaces[17] or needed additional dye wash-out steps in live cells.[16,22] In short, although impressive fluorescence enhancements have been reported *in vitro*, the ultimate purpose of fluorogenic probes, namely their application inside living cells under no-wash conditions, remains a challenge.

Herein, we report the synthesis of highly water-soluble fluorogenic xanthene tetrazine derivatives covering a wide emission range from green (fluorescein, Oregon Green) over yellow (tetramethylrhodamine) to far-red (Si-rhodamine). The novel tetrazine dyes were prepared *via* two highly modular synthetic routes. Furthermore, we successfully applied the new fluorogenic probes in selective protein labeling experiments. We demonstrate the usefulness of their fluorogenic properties by fluorescence microscopy imaging of the actin cytoskeleton in fixed cells as well as mitochondrial and nuclear proteins in living cells. To our knowledge, this is the first report of DA_{inv}-mediated no-wash protein imaging inside living cells utilizing fluorogenic tetrazines.

Results and discussion

We were guided by three design principles to exploit the advantages of fluorogenic tetrazine probes for live cell imaging:

Institut für Pharmazie und Molekulare Biotechnologie, Ruprecht-Karls-Universität Heidelberg, Im Neuenheimer Feld 364, 69120 Heidelberg, Germany. E-mail: wombacher@uni-heidelberg.de

† Electronic supplementary information (ESI) available: Synthetic procedures and spectroscopic data, details of cell experiments and imaging. See DOI: 10.1039/c6sc03879d

‡ These authors contributed equally.

first, the distance between the tetrazine, a chromophore itself, and the fluorophore is crucial for efficient quenching and the resulting fluorescence turn-on upon conversion in DA_{inv}. Therefore we developed new synthetic strategies to access fluorophore tetrazine probes with a minimal interchromophore distance. Tetrazine fluorogenic probes with ultra-short interchromophore distance have been reported for coumarins[18] and boron dipyrromethene (BODIPY) dyes.[17] However, coumarin and BODIPY fluorophores are not ideally suited for live cell imaging. Coumarins suffer from low brightness and the need of UV-light excitation. BODIPY dyes have limitations like low Stokes shifts and often poor aqueous solubility. Second, we aimed to focus on fluorophore classes that are preferentially used for intracellular live cell imaging. A common synthetic scheme to access tetrazine fluorophores involves the construction of the tetrazine moiety in the last synthetic step by converting nitriles with hydrazine in a classical Pinner-type reaction. Yet, this approach implies certain drawbacks. The harsh conditions of the Pinner tetrazine synthesis can result in product mixtures that are difficult to purify. Hence, our third aim was to find new synthetic methods to link tetrazines to fluorophores under mild conditions.

The derivatization of 1,2,4,5-tetrazines by various Pd-catalyzed cross-coupling reactions such as Stille,[23–25] Suzuki,[26,27] Sonogashira[25,28] and Heck[19] reactions as well as Buchwald–Hartwig aminations[27] has been described in literature. There are only few examples of C–C-bond formation at the 3- or 6-position of the tetrazine ring. Pop *et al.* have described the Stille coupling of 3,6-dichloro-1,2,4,5-tetrazine with an electron-rich tetrathiofulvalene tributylstannane.[29] This encouraged us to employ the Stille cross-coupling for the derivatization of tetrazines at the 3- and 6-positions. While being compatible with the base-sensitive tetrazine moiety, this chemistry further allows substitution directly at the tetrazine core, thereby giving access to a variety of tetrazine-based fluorogenic probes with minimal interchromophore distance. We identified 3-bromo-6-methyl-1,2,4,5-tetrazine **5** (ref. 30) as suitable building block for Stille cross-coupling chemistry. **5** can be synthesized in 5 steps starting from carbon disulfide and hydrazine monohydrate (Scheme S1†). Next, the fluorophore organotin derivatives for coupling with **5** were prepared from the corresponding aryl iodides or bromides. Halogen-substituted fluorescein and Oregon Green derivatives were MOM-protected (**7**, **11**, **15**) and converted to the organotin derivatives **8**, **12** and **16**. The critical cross-coupling of the fluorophore stannanes with **5** yielded the MOM-protected tetrazine probes **9**, **13** and **17** (Fig. 1, route I) which were deprotected to tetrazine dyes **Fl-5-Tz**, **Fl-6-Tz**, **OG-5-Tz** and **OG-6-Tz**. When transferred to rhodamine and Si-rhodamine substrates, the Stille coupling procedure described above did not give satisfactory results. Therefore, we established

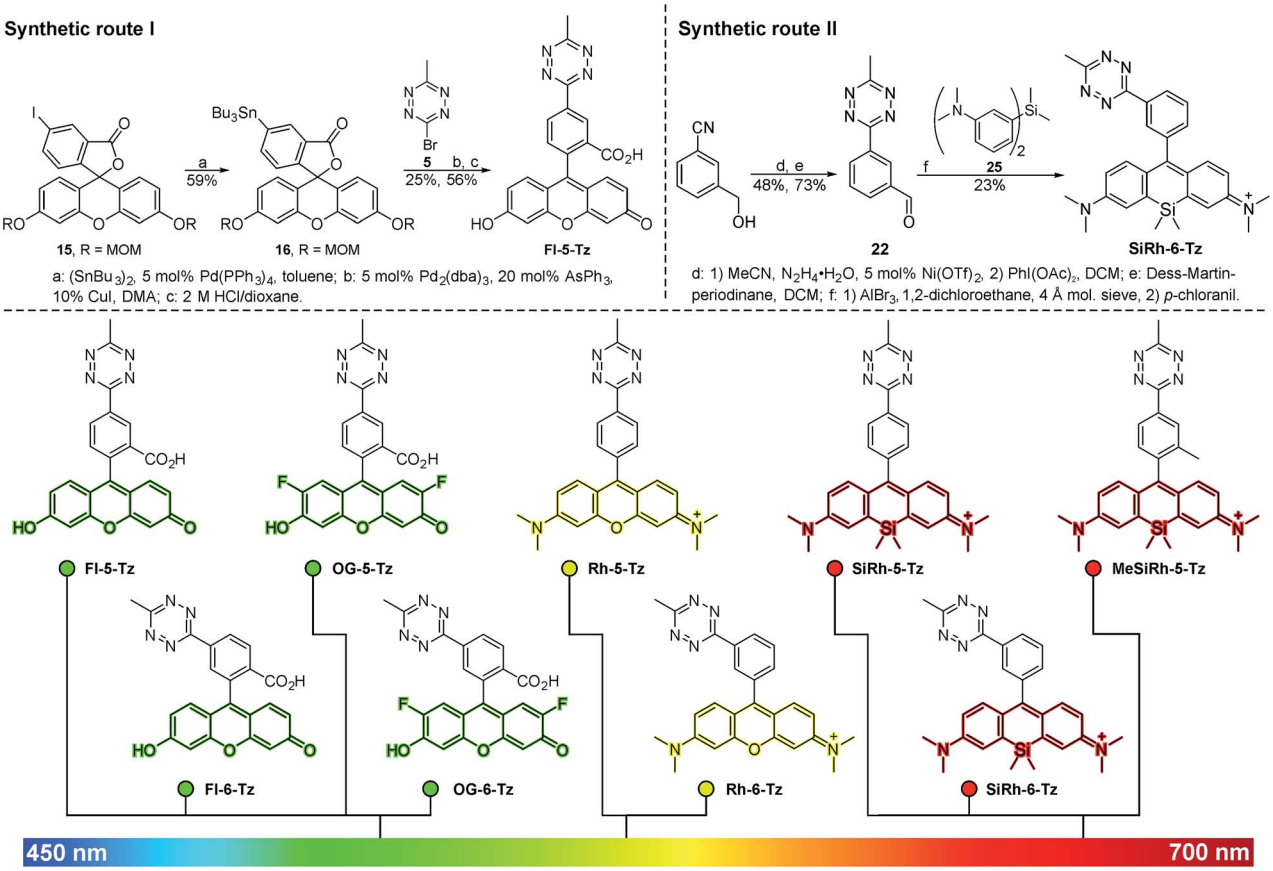

Fig. 1 Upper panel: Synthesis of fluorescein tetrazines *via* Pd-catalyzed Stille cross coupling (route I, left) and (Si-)rhodamine tetrazines using a Friedel Crafts alkylation followed by oxidation (route II, right). Lower panel: Green- to far-red-emitting fluorogenic xanthene tetrazines prepared in this study. Fluorescein and Oregon Green derivatives were synthesized according to route I, (Si-)rhodamines were accessible through route II.

an alternative synthetic strategy to gain access to more red-shifted tetrazine fluorophore probes. In literature, both the reaction of diarylethers[31] and diarylsilanes[32] with acid chlorides and aldehydes respectively to obtain (Si-)rhodamines have been described. We focused on aldehydes as electrophilic component and synthesized the required tetrazine benzaldehyde derivatives in a two-step procedure. First, commercially available or easily accessible hydroxymethyl benzonitrile derivatives were converted to the corresponding tetrazine benzylic alcohols **18**, **19** and **20**. These were mildly oxidized to the tetrazine benzaldehyde derivatives **21**, **22** and **23** using Dess–Martin periodinane. The aldehydes were subsequently reacted with diarylether **24** or diarylsilane **25** in a Friedel–Crafts alkylation. Subsequent oxidation with chloranil afforded the rhodamine tetrazines **Rh-5-Tz**, **Rh-6-Tz** and Si-rhodamine tetrazines **SiRh-5-Tz**, **SiRh-6-Tz** and **MeSiRh-5-Tz** (Fig. 1, route II). All newly synthesized tetrazine fluorogenic probes were photophysically characterized (Table 1, Fig. 2a), which required removal of fluorescent trace impurities by HPLC-purification. The fluorogenic properties were determined by conversion with *trans*-cyclooct-4-en-1-ol (TCO) in DA_{inv} (Table 1, Fig. 2c).

Fluorescence turn-on ratios of up to 109-fold for **Fl-6-Tz** were measured. As a general trend, the turn-on ratios were found to decrease with increasing emission wavelength. Though exhibiting quantum yields of the same magnitude as the yellow-emitting dyes, the Si-rhodamine tetrazines showed rather modest turn-on ratios (Table 1). Fluorescence quenching can be due to *e.g.* resonance energy transfer (RET) or Dexter interaction. Both energy transfer mechanisms are well known to be dependent on donor–acceptor spectral overlap.[33] The presence of such a process might explain the observed wavelength-dependent variation of the quenching efficiency for the herein presented tetrazine dyes. By monitoring the fluorescence increase over time, we found the cycloaddition to be finished within 10–15 min at equimolar reactant concentrations (Fig. 2b). The excellent aqueous solubility of all nine dyes makes the new fluorogenic tetrazines ideal candidates for application in biological environment. Having shown the potential of the synthesized dyes as fluorogenic probes, we were eager to evaluate their performance in cellular protein labeling experiments. First, we turned our focus to fixed cells and tested the probes for actin cytoskeleton staining. We used **phalloidin-TCO** to target the DA_{inv}-reactive TCO to actin filaments. Fixed HeLa cells were incubated with **phalloidin-TCO** and subsequently treated with either **OG-5-Tz**, **Rh-6-Tz** or **MeSiRh-5-Tz** and subjected to confocal imaging without previous dye wash-out. Phalloidin-specific labeling of filamentous structures was observed for all three fluorogenic dyes thereby covering a wide range of the visible spectrum (Fig. 3). Even though we observed low fluorescence turn-on *in vitro* for Si-rhodamine tetrazines, they proved to be well-suited for no-wash imaging (Fig. 3c). This indicates that there might be a cellular environmental effect on the Si-rhodamines' fluorescence properties, which has been previously reported by Lukinavičius *et al.*[34] for spirolactone-forming Si-rhodamines. When reacted with a TCO-modified model protein, **SiRh-5-Tz** and **MeSiRh-5-Tz** showed turn-on ratios that were up to three times higher than with TCO alone (Table 1, ESI†). This effect might be even more pronounced in cellular environment. In the absence of **phalloidin-TCO** no specific staining of actin filaments was observed (Fig. S5g–i†) with the tested tetrazine dyes.

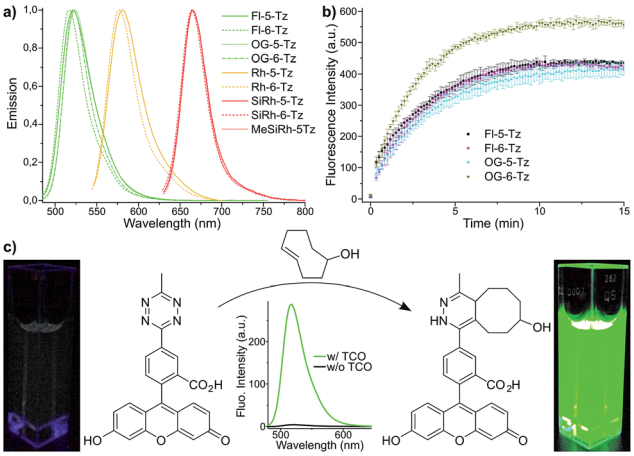

Fig. 2 (a) Normalized emission spectra of xanthene tetrazine derivatives. (b) Timecourse of fluorogenic DA_{inv} between green emitting tetrazine dyes and *trans*-cyclooct-4-en-1-ol (TCO) (500 nM in PBS each). (c) Fluorogenic reaction between **Fl-5-Tz** and TCO.

Table 1 Photophysical properties of the synthesized xanthene tetrazine dyes[a]

Dye	λ_{Abs} (nm)	λ_{Em} (nm)	ε_{max} (M^{-1} cm^{-1})	Φ_f	Turn-on (*x*-fold)
Fl-5-Tz	495	521	57 000	0.0037	72
Fl-6-Tz	495	517	55 000	0.0033	109
OG-5-Tz	495	524	87 000	0.0048	60
OG-6-Tz	495	522	70 000	0.0041	103
Rh-5-Tz	556	580	46 000	0.037	22
Rh-6-Tz	554	577	54 000	0.031	12
SiRh-5-Tz	650	665	58 000	0.020	1.8 (5.6)
SiRh-6-Tz	649	664	62 000	0.017	3.7
MeSiRh-5-Tz	651	666	53 000	0.026	2.0 (3.3)

[a] Φ_f denotes the relative fluorescence quantum yield of the unreacted dyes (for details see ESI†). Turn-on: fluorescence increase determined upon reaction of the dyes with TCO (values in brackets: reaction with TCO-labeled protein, see ESI) in PBS (pH 7.4).

To date, there are only few reports on tetrazine-mediated labeling inside living cells.[16,22,34–36] Yet successful target visualization required washing steps after addition of the tetrazine fluorophore. The herein reported new fluorogenic tetrazines enable no-wash imaging experiments inside living cells. We assumed that the OG-Tz dyes represent the best candidates for application in live cell labeling, as they combine high fluorescence turn-on rates in DA_{inv} with excellent photostability. Thus, we converted **OG-5-Tz** to its cell-permeable dipivalate ester derivative **OG-5-Tz(piv)$_2$**, which is hydrolyzed to the parent dye by endogenous esterases after having passed the cell membrane (Fig. 4a). For the labeling experiments HeLa cells expressing either mitochondrial Tom20-eDHFR (*E. coli* dihydrofolate reductase) or nuclear H2B-eDHFR were cultivated. We use the

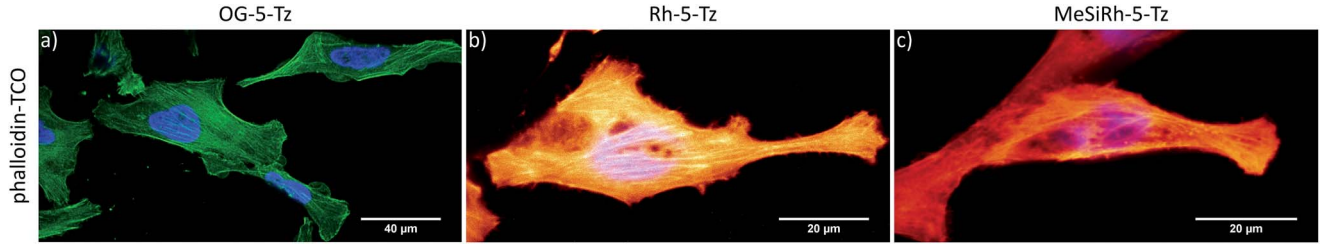

Fig. 3 No-wash fixed cell confocal imaging of actin cytoskeleton. HeLa cells were incubated with **phalloidin-TCO** (1 µg mL^{-1}), washed and treated with 10 µM **OG-5-Tz** (a), **Rh-5-Tz** (b) or **MeSiRh-5-Tz** (c). Hoechst 33342 was used as nuclear stain. Images were taken 30 min post addition of the dyes without previous dye-washout.

strong affinity of trimethoprim (TMP) to the eDHFR-tag to localize the DA_{inv}-reactive TCO* § (ref. 37) to the protein of interest (POI).[5,38] The cells were incubated with **TMP-TCO*** (10 µM, see ESI† for preparation) for 1 h, washed and **OG-5-Tz(piv)$_2$** (10 µM) was added. Confocal imaging showed fluorescent labeling of mitochondria (Fig. 4b–d) and nuclei respectively (Fig. 4e and S3†) indicating selective DA_{inv} of the fluorogenic dye with target-bound **TMP-TCO***. Despite omitting washing steps after addition of **OG-5-Tz(piv)$_2$**, only minimal background signal was observed, comparable to what we experienced from control experiments without **TMP-TCO*** (Fig. S5†). We also surveyed the stability of **OG-5-Tz** by incubation in PBS, cell lysate and in presence of glutathione and found the probe to be highly stable within the timescale of DA_{inv} (Fig. S1†). Labeling of the target structures was confirmed by colocalization with commercially available MitoTracker Red CMXRos (mitochondria) and Hoechst 33342 (nuclei), respectively. We also recorded the live cell labeling of nuclear H2B-eDHFR in real-time and observed good signal-to-noise ratio within 30 min (Fig. 4e). **OG-5-Tz(piv)$_2$** allows intracellular live cell labeling of POI fused to non-covalent domain tags (eDHFR tag) as well as POI carrying a covalent domain tag like HaloTag[39] (Fig. S4†).

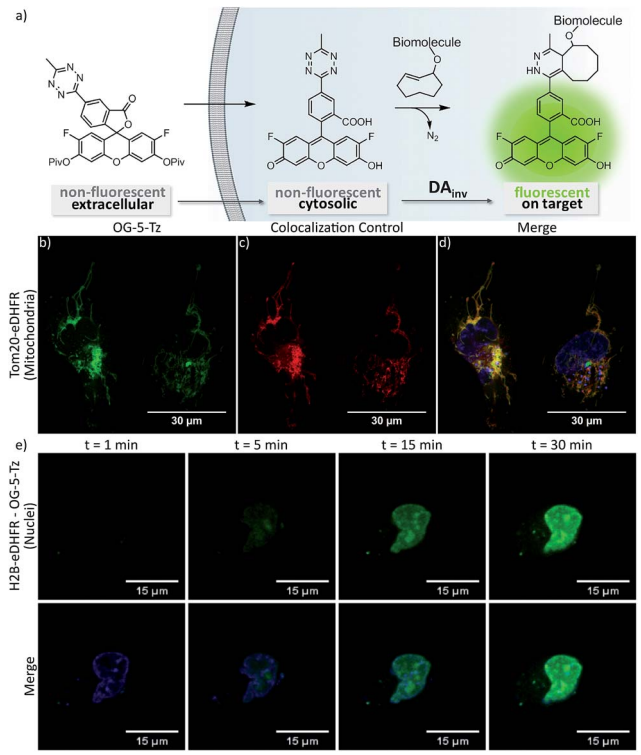

Fig. 4 Schematic representation of live cell labeling with **OG-5-Tz(piv)$_2$** (a). No-wash confocal live cell imaging of mitochondria (b–d) and timecourse of live cell nuclear labeling (e). Live HeLa cells expressing Tom20-eDHFR (b–d) or H2B-eDHFR (e) were incubated with **TMP-TCO*** (10 µM) and treated with 10 µM **OG-5-Tz(piv)$_2$**. MitoTracker Red CMXRos was used as mitochondrial colocalization control (c); Hoechst 33342 was used as nuclear colocalization control ((e): lower panel).

Conclusions

In conclusion, we have described two novel synthetic routes giving access to a variety of fluorogenic xanthene tetrazine derivatives ideally suited for applications in cell biology. The highly water-soluble dyes exhibit strong fluorescence enhancement upon conversion in DA_{inv} and cover a broad visible emission range going from green to far-red. We have demonstrated their potential in no-wash protein imaging in fixed and most notably inside living cells.

Acknowledgements

R. W. acknowledges funding from the Deutsche Forschungsgemeinschaft DFG (SPP1623, WO 1888/1-2). P. W. was supported by a Deutschlandstipendium and J. E. by a scholarship of the Foundation of German Business. We thank Dr Christian Ackermann, Dr Ulrike Engel and the Nikon Imaging Center for access to microscopes. We gratefully acknowledge Prof. Uwe Bunz for access to spectrophotometers.

Notes and references

§ Regioisomer of TCO with an improved stability towards *trans*/*cis*-isomerization in solution.

1 M. Fernandez-Suarez and A. Y. Ting, *Nat. Rev. Mol. Cell Biol.*, 2008, **9**, 929–943.
2 P. Shieh and C. R. Bertozzi, *Org. Biomol. Chem.*, 2014, **12**, 9307–9320.
3 A. Nadler and C. Schultz, *Angew. Chem., Int. Ed.*, 2013, **52**, 2408–2410.

4 A. Keppler, S. Gendreizig, T. Gronemeyer, H. Pick, H. Vogel and K. Johnsson, *Nat. Biotechnol.*, 2003, **21**, 86–89.
5 L. W. Miller, Y. Cai, M. P. Sheetz and V. W. Cornish, *Nat. Methods*, 2005, **2**, 255–257.
6 R. Wombacher and V. W. Cornish, *J. Biophotonics*, 2011, **4**, 391–402.
7 B. A. Griffin, S. R. Adams and R. Y. Tsien, *Science*, 1998, **281**, 269–272.
8 C. Uttamapinant, K. A. White, H. Baruah, S. Thompson, M. Fernández-Suárez, S. Puthenveetil and A. Y. Ting, *Proc. Natl. Acad. Sci. U. S. A.*, 2010, **107**, 10914–10919.
9 T. Plass, S. Milles, C. Koehler, J. Szymański, R. Mueller, M. Wießler, C. Schultz and E. A. Lemke, *Angew. Chem., Int. Ed.*, 2012, **51**, 4166–4170.
10 K. Lang, L. Davis, J. Torres-Kolbus, C. Chou, A. Deiters and J. W. Chin, *Nat. Chem.*, 2012, **4**, 298–304.
11 C. W. Tornøe, C. Christensen and M. Meldal, *J. Org. Chem.*, 2002, **67**, 3057–3064.
12 V. V. Rostovtsev, L. G. Green, V. V. Fokin and K. B. Sharpless, *Angew. Chem., Int. Ed.*, 2002, **41**, 2596–2599.
13 N. J. Agard, J. A. Prescher and C. R. Bertozzi, *J. Am. Chem. Soc.*, 2004, **126**, 15046–15047.
14 M. L. Blackman, M. Royzen and J. M. Fox, *J. Am. Chem. Soc.*, 2008, **130**, 13518–13519.
15 R. Pipkorn, W. Waldeck, B. Didinger, M. Koch, G. Müller, M. Wiessler and K. Braun, *J. Pept. Sci.*, 2009, **15**, 235–241.
16 N. K. Devaraj, S. Hilderbrand, R. Upadhyay, R. Mazitschek and R. Weissleder, *Angew. Chem., Int. Ed.*, 2010, **49**, 2869–2872.
17 J. C. Carlson, L. G. Meimetis, S. A. Hilderbrand and R. Weissleder, *Angew. Chem., Int. Ed.*, 2013, **52**, 6917–6920.
18 L. G. Meimetis, J. C. T. Carlson, R. J. Giedt, R. H. Kohler and R. Weissleder, *Angew. Chem., Int. Ed.*, 2014, **53**, 7531–7534.
19 H. Wu, J. Yang, J. Seckute and N. K. Devaraj, *Angew. Chem., Int. Ed.*, 2014, **53**, 5805–5809.
20 G. Knorr, E. Kozma, A. Herner, E. A. Lemke and P. Kele, *Chem. - Eur. J.*, 2016, **22**, 8972–8979.
21 P. Shieh, V. T. Dien, B. J. Beahm, J. M. Castellano, T. Wyss-Coray and C. R. Bertozzi, *J. Am. Chem. Soc.*, 2015, **137**, 7145–7151.
22 D. S. Liu, A. Tangpeerachaikul, R. Selvaraj, M. T. Taylor, J. M. Fox and A. Y. Ting, *J. Am. Chem. Soc.*, 2012, **134**, 792–795.
23 J. Sołoducho, J. Doskocz, J. Cabaj and S. Roszak, *Tetrahedron*, 2003, **59**, 4761–4766.
24 Z. Li, J. Ding, N. Song, J. Lu and Y. Tao, *J. Am. Chem. Soc.*, 2010, **132**, 13160–13161.
25 A. Wieczorek, T. Buckup and R. Wombacher, *Org. Biomol. Chem.*, 2014, **12**, 4177–4185.
26 F. Suzenet, N. Leconte, A. Keromnes-Wuillaume and G. Guillaumet, *Synlett*, 2007, **2007**, 0204–0210.
27 C. Quinton, V. Alain-Rizzo, C. Dumas-Verdes, G. Clavier, L. Vignau and P. Audebert, *New J. Chem.*, 2015, **39**, 9700–9713.
28 Z. Novak and A. Kotschy, *Org. Lett.*, 2003, **5**, 3495–3497.
29 F. Pop, J. Ding, L. M. L. Daku, A. Hauser and N. Avarvari, *RSC Adv.*, 2013, **3**, 3218.
30 A. D. Counotte-Potman and H. C. van der Plas, *J. Heterocycl. Chem.*, 1978, **15**, 445–448.
31 A. V. Anzalone, T. Y. Wang, Z. Chen and V. W. Cornish, *Angew. Chem., Int. Ed.*, 2013, **52**, 650–654.
32 B. Wang, X. Chai, W. Zhu, T. Wang and Q. Wu, *Chem. Commun.*, 2014, **50**, 14374–14377.
33 S. Hassoon, H. Lustig, M. B. Rubin and S. Speiser, *J. Phys. Chem.*, 1984, **88**, 6367–6374.
34 G. Lukinavičius, K. Umezawa, N. Olivier, A. Honigmann, G. Yang, T. Plass, V. Mueller, L. Reymond, I. R. Corrêa Jr, Z.-G. Luo, *et al.*, *Nat. Chem.*, 2013, **5**, 132–139.
35 R. S. Erdmann, H. Takakura, A. D. Thompson, F. Rivera-Molina, E. S. Allgeyer, J. Bewersdorf, D. Toomre and A. Schepartz, *Angew. Chem., Int. Ed.*, 2014, **53**, 10242–10246.
36 F. Doll, A. Buntz, A.-K. Späte, V. F. Schart, A. Timper, W. Schrimpf, C. R. Hauck, A. Zumbusch and V. Wittmann, *Angew. Chem., Int. Ed.*, 2016, **55**, 2262–2266.
37 I. Nikić, T. Plass, O. Schraidt, J. Szymański, J. A. G. Briggs, C. Schultz and E. A. Lemke, *Angew. Chem., Int. Ed.*, 2014, **53**, 2245–2249.
38 R. Wombacher, M. Heidbreder, S. van de Linde, M. P. Sheetz, M. Heilemann, V. W. Cornish and M. Sauer, *Nat. Methods*, 2010, **7**, 717–719.
39 G. V. Los, L. P. Encell, M. G. McDougall, D. D. Hartzell, N. Karassina, C. Zimprich, M. G. Wood, R. Learish, R. F. Ohana, M. Urh, *et al.*, *ACS Chem. Biol.*, 2008, **3**, 373–382.